
Article:
Wagg, D.J. (2003) Periodic and chaotic dynamics in an asymmetric elastoplastic oscillator. Chaos, Solitons and Fractals, 16 (5). 779 - 786. ISSN 0960-0779

https://doi.org/10.1016/S0960-0779(02)00437-X

Chaos, Solitons & Fractals, (2003), 16: 779786

Periodic and chaotic dynamics in an asymmetric elastoplastic oscillator

D. J. Wagg

Department of Mechanical Engineering, University of Bristol, Queens Building, University Walk, Bristol BS8 1TR, U.K.

May 3, 2013

Abstract

We consider the dynamics of a harmonically forced oscillator with an asymmetric elastic–perfectly plastic stiffness function. The computed bifurcation diagrams for the oscillator show regions of periodic motion, hysteresis and large regions of chaotic motion. These different regions of dynamical behaviour are plotted in a two dimensional parameter space consisting of forcing amplitude and forcing frequency. Examples of the chaotic motion encountered are shown using a discontinuity crossing map. Comparisons are made with the symmetric oscillator by computing a typical bifurcation diagram and considering previously published results for the symmetric system. From this we conclude that the asymmetric system is dominated by a large region of chaotic motion whereas in the symmetric oscillator period one motion and coexisting period three motion predominates.

1 Introduction

In this paper we consider the occurance of periodic and chaotic regions in systems with symmetric and asymmetric elastoplastic stiffness characteristics. In particular, we consider the behaviour of an oscillator, with an idealised elastic–perfectly plastic stiffness. This type of stiffness function is an often used idealisation of hysteretic material behaviour which gives a piecewise linear softening spring function. The piecewise linear nature of the stiffness means that the overall function is nonsmooth, and hence the associated dynamics are strongly nonlinear. However the hysteretic function is nearly always assumed to be symmetric. Here we consider breaking the symmetry by considering an asymmetric one–sided stiffness function. These results are compared with simulations of systems with symmetric elastic–perfectly plastic stiffness.

The behaviour of elastic-plastic structures has been considered by many authors, for a recent treatment see [1] and the references therein. A one dimensional mapping derived from a single degree of freedom system with elastic-plastic stiffness has been considered by Miller & Butler [2]. This approach follows the work on nonsmooth dynamical systems of Shaw & Holmes [3], for single degree of freedom systems. Capecchi [4] has studied the elastoplastic oscillator using a nonsmooth mapping approach. Capecchi and others [5, 6, 7] have extended this approach to two degree of freedom hysteretic oscillators. This work has relevance to structural engineering, particularly earthquake engineering, because most structural systems have a hysteretic response to large amplitude excitations. Capecchi *et al.* [8] have considered using nonparametric models to identify the hysteresis present during earthquake excitation.

More general piecewise linear single degree of freedom systems have also been considered by Thompson *et al.* [9] and Natsiavas [10]. Applying such techniques to multi degree of freedom systems has been considered by several authors including Nigm *et al.* [11] and Natsiavas [12].

In section 2 we consider the equations of motion of a harmonically forced single degree of freedom oscillator with symmetric and asymmetric elastoplastic stiffness characteristics. Then in section 3 we consider the bifurcation diagrams and phase portraits for the asymmetric oscillator. Examples of chaotic motions are considered using a discontinuity crossing map [2, 4]. Then we consider the regions of periodic and chaotic motion in a two dimensional parameter space of forcing amplitude and forcing frequency. These results are compared with those of Miller & Butler [2] who computed the results for the symmetric case. We also compare a typical bifurcation diagram for the symmetric and asymmetric cases. All the simulations computed here show steady state dynamics so that direct comparison with the results of Miller & Butler [2] can be made. We note that for specific application to structural dynamics problems transient effects may also be significant.

2 Equations of motion

We consider equations of motion which represent an idealised single degree of freedom oscillator.

$$m\ddot{x} + c\dot{x} + \phi(x) = A\cos(\Omega t), \tag{1}$$

where m represents mass, c represents viscous damping, A is the forcing amplitude, Ω is the forcing frequency and an overdot represents differentiation with respect to time t. We can define a stiffness function ϕ for the symmetric case as

$$\phi(x) = \begin{cases} -P^* & \text{for} \quad x < -x_p \\ kx & \text{for} \quad -x_p < x < x_p \\ P^* & \text{for} \quad x > x_p \end{cases}, \tag{2}$$

where k is the linear stiffness and P^* the plastic yield force. For the asymmetric case, we define a one sided stiffness function

$$\hat{\phi}(x) = \begin{cases} kx & \text{for} \quad x < x_p \\ P^* & \text{for} \quad x > x_p \end{cases}, \tag{3}$$

We can recast equation 2 in a nondimensional formulation by defining $y = x/x_p$, $\zeta = c/2m\omega_n$, $\omega_n = \sqrt{k/m}$ and $\tau = \omega_n t$. Then equation 2 can be written as

$$\ddot{y} + 2\zeta\dot{y} + \phi(y) = F\cos(\omega\tau), \tag{4}$$

where a dot now denotes differentiation with respect to nondimensional time τ, $F = A/(kx_p)$ nondimensional forcing amplitude, $\omega = \Omega/\omega_n$ is the nondimensional frequency ratio and

$$\phi(y) = \begin{cases} -1 & \text{for} \quad y < -1 \\ y & \text{for} \quad -1 < y < 1 \\ 1 & \text{for} \quad y > 1 \end{cases}, \tag{5}$$

by using the relation $P^* = kx_p$. The corresponding nondimensionalised stiffness for the asymmetric case is

$$\hat{\phi}(y) = \begin{cases} y & \text{for} \quad y < 1 \\ 1 & \text{for} \quad y > 1 \end{cases}. \tag{6}$$

We can compute the boundary between elastic and plastic behaviour for harmonic forcing functions in the following manner. In the elastic region equation 4 can be written as the standard second order differential equation

$$\ddot{y} + 2\zeta\dot{y} + y = F\cos(\omega\tau). \tag{7}$$

The steady state solution of equation 7 can be written as

$$y = \frac{F}{\Delta}\cos(\omega\tau - \psi), \tag{8}$$

where $\Delta = ((1-\omega^2)^2 + 4\zeta^2\omega^2)^{1/2}$ and $\psi = \arctan(2\zeta\omega/(1-\omega^2))$ is the phase of the oscillator. For any particular steady state solution the maximum amplitude will occur when $\cos(\omega\tau - \psi) = 1$. When the limit of elastic behaviour is reached $y = 1$, so that equation 8 can be rearranged to give

$$F = ((1-\omega^2)^2 + 4\zeta^2\omega^2)^{1/2}. \tag{9}$$

This expression defines a curve in F, ω parameter space which represents the limit of elastic behaviour for the oscillator.

3 Numerical results

We now consider the dynamics of the single degree of freedom system as parameters are varied. In this study, we will use the frequency ratio, ω and nondimensional forcing amplitude F as the variable parameters. This will allow us to study the behaviour of the system in a region of F, ω space centred around the system natural frequency $\omega = 1$ and for the forcing amplitude range $0 < F \leq 10$. The simulations were computed by integrating the equation of motion, equation 7, using a 4th order Runge-Kutta algorithm. At the nonsmooth change in stiffness, the time of change was located by root finding using a secant method. Each of the simulations was started with zero initial conditions.

The bifurcation diagrams for steady state behaviour were computed by allowing 100 periods of transient motion to elapse before recording 30 periods of steady state motion. In addition, the parameters were varied from zero to a final value, and then back to zero again, in order to locate any multiple solutions or regions hysteretic behaviour.

A typical set of results from this type of analysis for the symmetric case is shown in figure 1, where the parameter variation with forcing amplitude is shown, when the frequency ratio $\omega = 1$ and $\zeta = 0.05$. We observe from figure 1, that the there two coexisting periodic solutions. The first solution is a period one response which is close to bilinear. This consists of an initial linear elastic response up to a forcing amplitude of $F \approx 0.2$, at which point the elastic limit is reached, so that for amplitudes $F > 0.2$ the orbit spends some time in the plastic region. The second solution is a period three solutions which exists between $F \approx 3.5$ and $F \approx 8.7$. A very small region of non-periodic behaviour can be observed following the period three solution at $F \approx 8.7$.

A bifurcation diagram of the single degree of freedom asymmetric case with $\omega = 1.0$

is shown in figure 2. As before, the initial response is linear elastic period one motion up to $F \approx 0.2$. The period one motion continues with asymmetric elastic–plastic behaviour up to $F \approx 1.38$ where a period doubling bifurcation occurs. Then, for increasing F, at $F \approx 2.085$ there is a sudden transition to chaotic motion. Between $1 < F < 2.085$ a region of hysteretic behaviour exists, with coexisting periodic solutions.

In figure 3 phase portraits for a selection of forcing amplitudes are shown for the asymmetric case for $\omega = 1.0$. Figure 3 (a) shows the phase portrait for the oscillator after the elastic limit is reached, at $F = 0.5$. We observe from figure 3 (b)–(f), that a range of other periodic and chaotic motions occur, in the parameter range considered. These motions can be characterised by considering the map between successive crossings of the nonsmooth stiffness discontinuity. e.g. if Σ defines the hyperplane in phase space when $|y| = 1$ (in fact for the asymmetric case we need only the condition $y = 1$) such that $\Sigma = \{(y, \dot{y}, t) \in \mathbb{R}^3 : y = 1\}$, then the mapping $h : \Sigma \to \Sigma$, is the discontinuity crossing map, which is defined by the time and velocity, $\dot{y}$, of crossing. It is convenient for harmonic forcing to consider the time of crossing modulo the forcing frequency, which we define as $\varphi = \tau \bmod 2\pi/\omega$. Using these definitions the map for the chaotic attractor shown in figure 3 (c) with $F = 4.0$, $\omega = 1.0$ has be computed, and is shown in figure 4. In this figure we observe that the structure of the attractor has similarities with attractors found in other nonsmooth systems [13], in that the attractor is composed of linear sets. For higher frequency values the chaotic attractor the chaotic attractor appears to have a qualitatively different structure but again is composed mainly of linear sets. The discontinuity crossing map is shown in figure 5 for $F = 0.4$ and $\omega = 1.75$.

A full set of bifurcation diagrams for the asymmetric case is shown in figure 6. Here we see that at low frequency, $\omega = 0.25$, the chaotic region has large periodic windows within it. These large periodic windows period add by one as F increases. A few much smaller periodic window exist between the larger windows. As ω increases the periodic window

reduce in size until at $\omega = 1.5$ no periodic windows exist within the chaotic region. We note also that at low frequency values the response amplitudes are very large, e.g. at $\omega = 0.25$ the maximum amplitudes are in excess of $y = 700$. Whereas at $\omega = 0.75$ the maximum amplitudes are of the order $y = 10$.

Another significant feature of the diagrams shown in figure 6 are the hysteretic regions. For example in figure 6 (b), between $F \approx 0.5$ and $F \approx 1.1$ there period one solution has two coexisting solutions. Similar regions of hysteretic behaviour, containing other periodic solutions typically period 1 and 2, exist for all the bifurcation diagrams shown in figure 6, along with many other hysteretic regions which overlap with chaotic regions.

For the asymmetric stiffness case we can summarise the periodic and chaotic regions in the F, ω parameter space. This is shown in figure 7, where the solid line represents the limit of elastic behaviour. Therefore the region below the solid line represents parameter values which lead to purely elastic steady state behaviour. We note that it is also possible for the the elastic limit to be reached during transient motion for certain initial conditions within the the elastic region $-1 < y < 1$, however here we are starting with $F, \omega \ll 1$ and increasing parameters slowly after transients have decayed away. Close to the natural frequency, $\omega = 1$, a region of stable period one (P1) motions exist above the elastic limit line. These motions then loose stability via a period doubling bifurcation which leads to a region of period two and higher period n (Pn) periodic motions. Eventually for increasing F values chaotic motion with periodic windows predominates. The chaotic region is bounded for increasing ω such that at $\omega = 2$ period one motion exists for the whole range of forcing amplitude values considered. For very low frequencies the chaotic region is again bounded. For clarity we have omitted the hysteretic regions from figure 7.

In figure 8 we show a similar region of F, ω parameter space for the symmetric case. Here the dominant motions are period one (P1) and period three (P3) motions, which coexist for large regions of the parameter space considered. For frequency values below

$\omega = 0.75$ the basin of attraction for the period three motion is very small, so solutions have not been sought below this value. There are small regions of non-periodic motion for the symmetric case which occur within the coexisting period 3 region shown in figure 8. There is also a region of coexisting period three and elastic solutions for frequencies above $\omega \approx 1.79$.

4 Conclusions

In this paper we have discussed the periodic, chaotic and hysteretic behaviour which occurs in an asymmetric elastoplastic oscillator. The main result is that in the asymmetric oscillator case the dominant motion is chaotic in the region of interest close the the natural frequency of the system. Conversely for symmetric elastoplastic systems previous authors (e.g. see [2]) have shown that the dominant motion in the F, ω space close to $\omega = 1$ is stable period one motion. In this paper we have noted from a typical bifurcation diagram of the symmetric oscillator that it is possible for other solutions (in this case period 3) to coexist with the dominant period one motions. Figure 8 shows that the region of coexisting period three motion is significant in size. The asymmetric stiffness function has generally less applications than the symmetric case for modelling structural dynamics, however it does demonstrate that by breaking the symmetry of the system the complexity of the subsequent dynamics will be increased.

References

[1] U. Lepik. On dynamic buckling of elastic-plastic beams. *International Journal of Non-linear Mechanics*, 35:721–734, 2000.

[2] G. R. Miller and M. E. Bulter. Periodic response of elastic-perfectly plastic sdof oscillator. *Journal of Engineering Mechanics ASCE*, 114(3):536–550, 1988.

[3] S. W. Shaw and P. J. Holmes. A periodically forced piecewise linear oscillator. *Journal of Sound and Vibration*, 90(1):129–155, 1983.

[4] D. Capecchi. Asymptotic motions and stability of the elastoplastic oscillator studied via maps. *Journal of Solids and Structures*, 30(23):3303–3314, 1993.

[5] D. Capecchi, R. Masiani, and F. Vestroni. Periodic and non-periodic oscillations of a class of hysteretic two degree of freedom systems. *Nonlinear Dynamics*, 13:309–325, 1997.

[6] D. Capecchi and F. Vestroni. Asymptotic response of a two degree of freedom system under harmonic excitation. internal resonance case. *Nonlinear Dynamics*, 7:317–333, 1995.

[7] S. V. Sorokin, A. V. Terentiev, and B. L. Karihaloo. Nonlinear dynamics and stability of a two d.o.f. elastic/elasto–plastic model system. *Meccanica*, 34:311–336, 1999.

[8] F. Benedettini, D. Capecchi, and F. Vestroni. Identification of hysteretic oscillators under earthquake loading by nonparametric models. *ASCE:Journal of Engineering Mechanics*, 121(5):606–612, 1995.

[9] J. M. T. Thompson, A. R. Bokaian, and R. Ghaffari. Subharmonic resonances and chaotic motions of a bilinear oscillator. *Journal of Applied Mathematics*, 31:207–234, 1983.

[10] S. Natsiavas and H. Gonzalez. Vibration of harmonically excited oscillators with asymmetric constraints. *Journal of Applied Mechanics*, 59:284–290, 1992.

[11] M. M. Nigm and A. A. Shabana. Effect of an impact damper on a multi-degree of freedom system. *Journal Of Sound and Vibration*, 89(4):541–557, 1983.

[12] S. Natsiavas. Dynamics of multiple-degree-of-freedom oscillators with colliding components. *Journal of Sound and Vibration*, 165(3):439–453, 1993.

[13] C. J. Budd and F. Dux. Intermittency in impact oscillators close to resonance. *Nonlinearity*, 7:1191–1224, 1994.

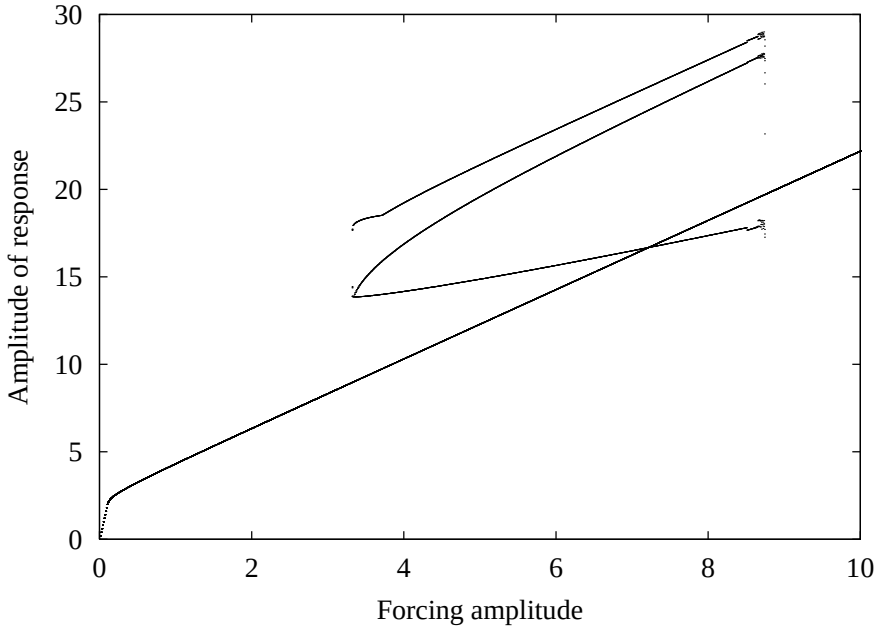

Figure 1: Bifurcation diagram of single degree of freedom symmetric elastic-perfectly plastic system obtained by varying forcing amplitude, F. Parameter values $\zeta = 0.05$, $\omega = 1.0$.

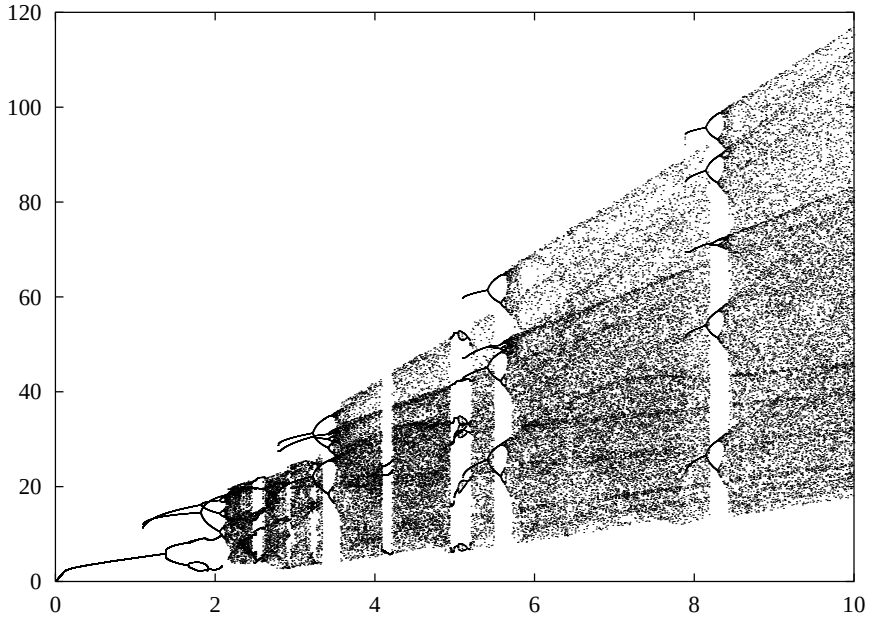

Figure 2: Bifurcation diagram of single degree of freedom asymmetric elastic-perfectly plastic system obtained by varying forcing amplitude, F. Parameter values $\zeta = 0.1$, $\omega = 1.0$.

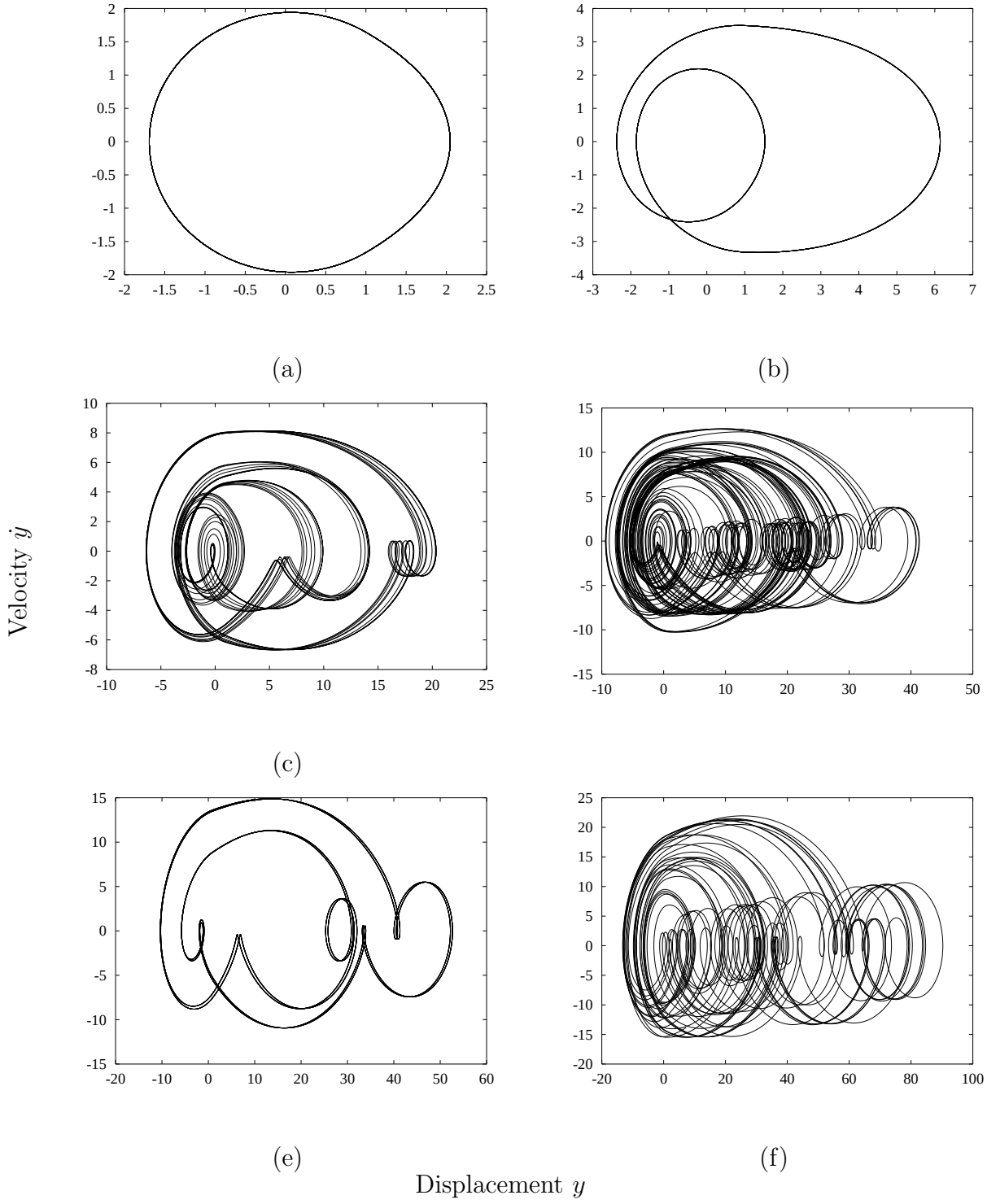

Figure 3: Numerically computed phase portraits for an asymmetric single degree of freedom elastic-plastic oscillator. Parameter values $\zeta = 0.05$, frequency $\omega = 1.0$ forcing amplitude (a) $F = 0.5$ (b) $F = 1.5$ (c) $F = 2.5$ (d) $F = 4.0$ (e) $F = 5.0$ (f) $F = 8.0$.

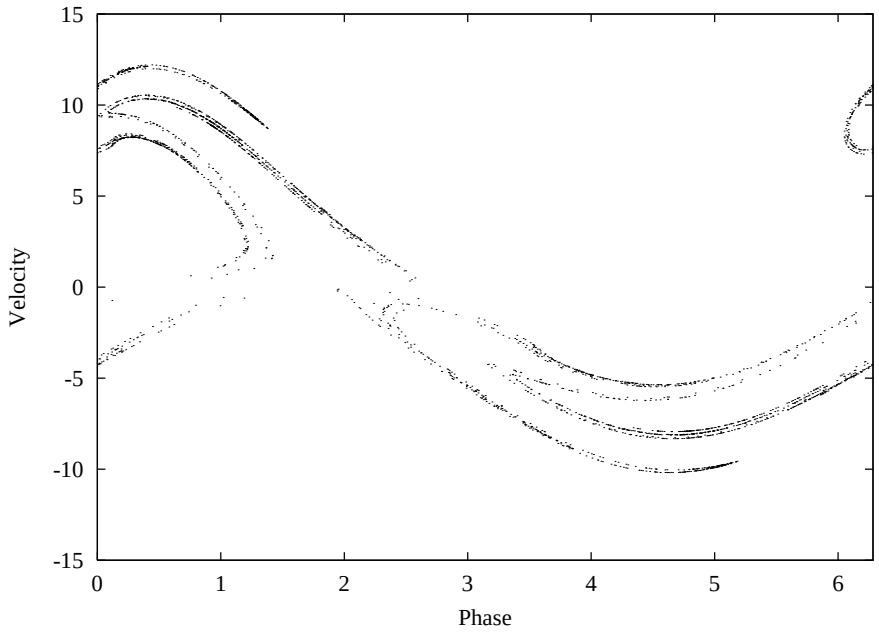

Figure 4: Discontinuity crossing map of chaotic attractor at parameter values $\zeta = 0.05$, $F = 4.0$,$\omega = 1.0$.

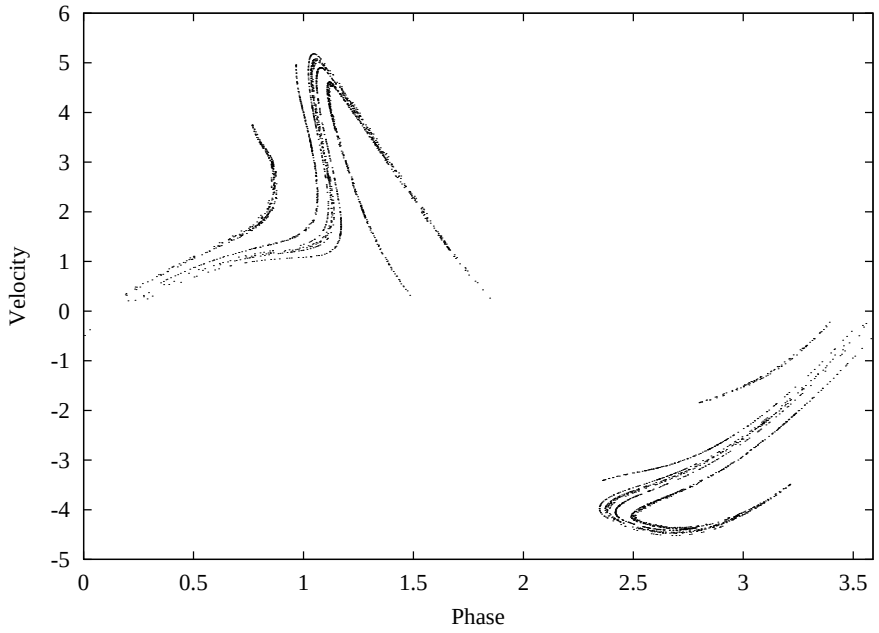

Figure 5: Discontinuity crossing map of chaotic attractor at parameter values $\zeta = 0.05$, $F = 4.0$, $\omega = 1.75$.

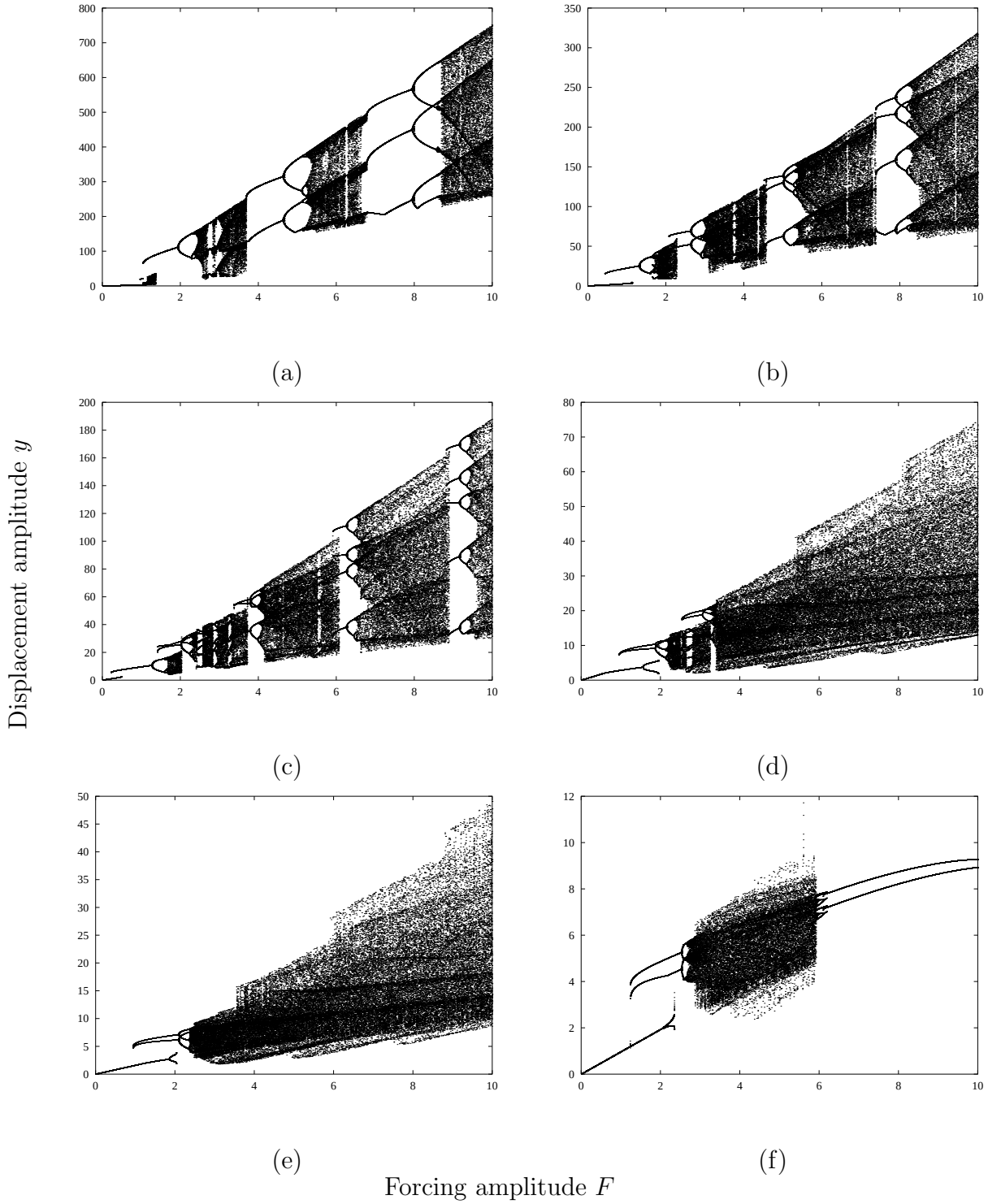

Figure 6: Numerically computed bifurcation diagrams for an asymmetric single degree of freedom elastic-plastic oscillator. Parameter values $\zeta = 0.05$, and (a) $\omega = 0.25$ (b) $\omega = 0.5$ (c) $\omega = 0.75$ (d) $\omega = 1.25$ (e) $\omega = 1.5$ (f) $\omega = 1.75$.

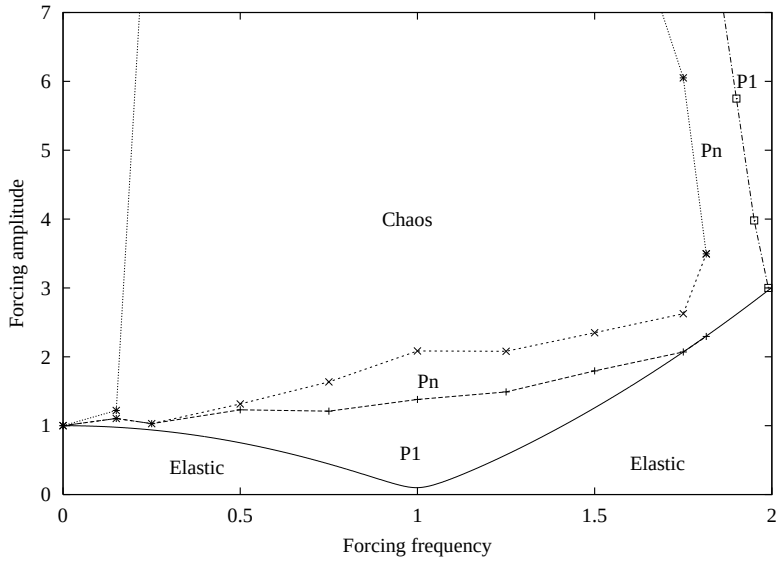

Figure 7: Asymmetric case. Regions of dominant motion in $F - \omega$ parameter space.

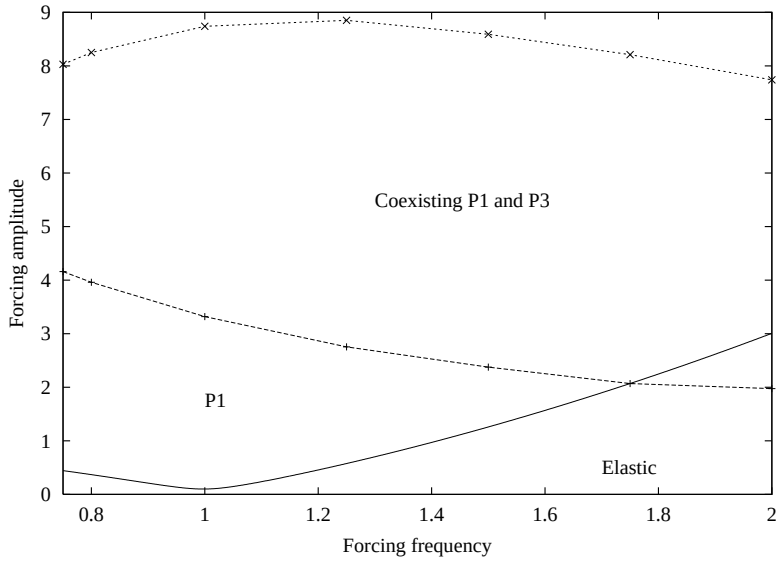

Figure 8: Symmetric case. Regions of dominant motion in $F - \omega$ parameter space.